

Immobilization of fluorescent protein TagGFP2 on Fe₃O₄-based magnetic nanoparticles*

A. M. Demin,^{a*} M. S. Valova,^a A. G. Pershina,^{b,c} and V. P. Krasnov^a

^aI. Ya. Postovsky Institute of Organic Synthesis, Ural Branch of the Russian Academy of Sciences, 22 ul. S. Kovalevskoi, 620137 Ekaterinburg, Russian Federation.

Fax: +7 (343) 374 1189. E-mail: demin@ios.uran.ru

^bSiberian State Medical University,

2/18 Moskovsky trakt, 634050 Tomsk, Russian Federation

^cNational Research Tomsk Polytechnic University,

30 prosp. Lenina, 634050 Tomsk, Russian Federation

The immobilization of fluorescent protein TagGFP2 on Fe₃O₄-based magnetic nanoparticles (MNPs), preliminarily functionalized with 3-aminopropylsilane and *N*-(phosphonomethyl) iminodiacetic acid (PMIDA), was studied. Protein binding to MNPs depending on the nature of the surface functional groups, the medium, and the presence of a coupling agent, namely, 1-(3-dimethylaminopropyl)-3-ethylcarbodiimide (EDC), was studied using fluorimetry, UV and IR spectroscopy. It was shown that protein immobilization can occur by both non-covalent and covalent binding with surface groups of MNPs. The best results (up to 150 μg of TagGFP2 per 1 mg of MNPs) were obtained for MNPs preliminarily functionalized with PMIDA and using EDC. The results of this study can be used for the design of imaging agents having both magnetic and optical properties to be applied in biomedicine.

Key words: magnetic nanoparticles, TagGFP2, fluorimetry, UV spectroscopy.

At present, nanomaterials based on Fe₃O₄ magnetic nanoparticles (MNPs) are used as diagnostic and therapeutic agents, as a platform for drug delivery and separation of biomolecules or cells.^{1–3} The Fe₃O₄ nanoparticles have high magnetic properties, are efficient *T*₂-contrast agents** in MRI studies, can be easily functionalized for further conjugation with organic molecules, they are biocompatible and biodegradable.⁴ Of particular interest are nanomaterials with magnetic and optical properties (for example, those based on Fe₃O₄ MNPs and quantum dots).^{5–7}

Green fluorescent protein (GFP) is highly biocompatible in comparison with quantum dots, has good fluorescent properties, and can be used to synthesize nanoconjugates with MNPs. Fluorescent proteins are often used as model objects in the development of systems for isolation and purification of His6-tagged recombinant proteins. For this, the His6-GFP protein reversibly binds to Cu²⁺

(see Ref. 8) or Ni²⁺ ions (see Ref. 9) preliminarily deposited on the modified surface of Fe₃O₄ MNPs or to nanoparticles based on Ni/NiO¹⁰ and Fe₃O₄/NiO.¹¹

The fluorescent properties of proteins of the GFP family make it possible to visualize the binding of other protein molecules (expressed as a fusion partners with GFP) to the nanoparticle surface and to estimate their quantity. For example, during the development of a biosensor system, a recombinant protein fused with TagGFP was used to visualize the site-specific conjugation of the protein TagSNAP with the surface of a modified Au substrate.¹² In addition, GFP was used to label A54 peptide (possesses a high specificity toward hepatocarcinoma cells), which was subsequently immobilized on MNPs.¹³ In this study, we used the recombinant protein TagGFP2 (pI 5.73).¹⁴ The protein TagGFP2 is characterized by a bright fluorescence, a high pH value, and photostability. An additional advantage of the protein TagGFP2 is its existence in a monomeric form and the possibility of its successful use as a fluorescent tag for biomedical purposes, for example, for visualizing cells in the *in vitro* experiments.

The goal of this work is to study the non-covalent and covalent (using 1-(3-dimethylaminopropyl)-3-ethylcarbodiimide (EDC) as a coupling agent) immobilization processes of the fluorescent protein TagGFP2 on MNPs containing surface carboxy or amino groups, depending

* Based on the materials of the IV Interdisciplinary Symposium on Medicinal, Organic, Biological Chemistry and Pharmaceutics (MOBI-ChemPharma 2018) (September 23–26, 2018, Novyi Svet, Crimea).

** Agents used for magnetic resonance imaging (MRI), which allow to enhance the contrast of the resulting tissue image by changing the transverse relaxation time (*T*₂) of protons of water molecules surrounding this contrast agent.

on the nature of the reaction medium (water or phosphate-buffered saline (PBS)).

Results and Discussion

In this work, we used Fe₃O₄-based MNPs with a diameter of 11 nm,^{15,16} obtained by deposition from solutions of Fe³⁺ and Fe²⁺ salts. In order to form functional groups on the surface of MNPs allowing subsequent covalent binding with the protein, we modified the starting MNPs with *N*-(phosphonomethyl) iminodiacetic acid monohydrate (PMIDA)^{17,18} or (3-aminopropyl)trimethoxysilane (APTMS)^{15,16} as shown in Scheme 1. As a result, MNPs containing carboxy (**1**) or amino groups (**2**) on the surface were obtained (see Scheme 1). Previously, both types of modified MNPs were demonstrated to be suitable for use as *T*₂-contrast enhancing agents when performing MRI diagnostics of liver in the *in vivo* experiments.^{16,18,19}

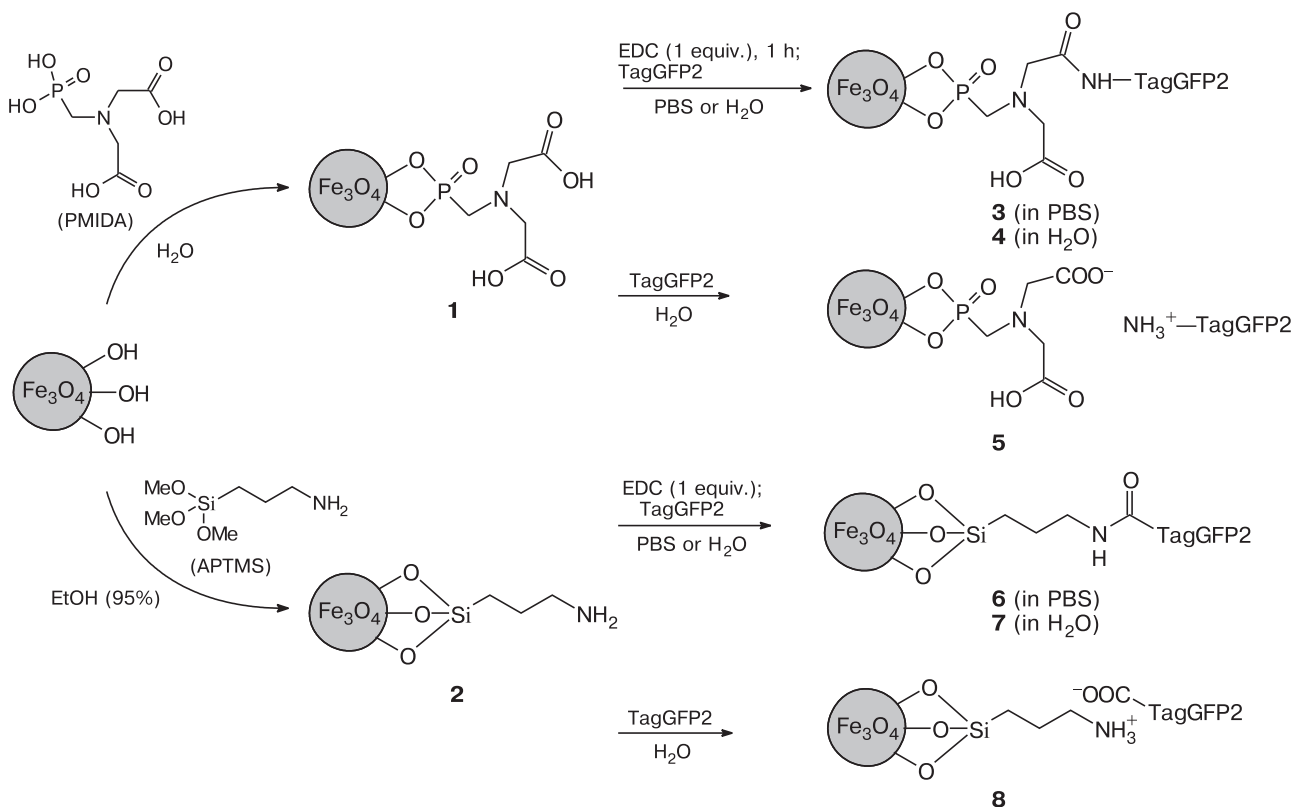
The amount of PMIDA and APS attached to MNPs was calculated according to the mass fraction of carbon determined based on elemental analysis. The amount of APS was also determined by IR spectroscopy.²⁰ Thus, for MNPs **1** the amount of PMIDA was 0.57 mmol g⁻¹ of MNPs (or 1.14 mmol g⁻¹ of MNPs calculated based on the number of carboxy groups), for MNPs **2** the amount of amino groups was 0.60 mmol g⁻¹ of MNPs.

The immobilization of TagGFP2 can occur either by non-covalent surface sorption or by coupling of carboxy or amino groups on the surface of synthesized MNPs to the free amino or carboxy groups of the protein, respectively, when using water-soluble carbodiimide EDC.

The TagGFP2 used in this work has excellent fluorescent properties ($\lambda_{\text{Ex}} = 460$ nm and $\lambda_{\text{Em}} = 506$ nm), with a relative quantum yield of 0.65 (with a standard fluorescein, $\lambda_{\text{Ex}} = 460$ nm) (Fig. 1), therefore, it is convenient to study its immobilization on MNPs using fluorescence spectroscopy. A graph of fluorescence intensity *versus* protein concentration in solution was plotted to evaluate the degree of protein immobilization on MNPs based on its residue in the reaction mixture (Fig. 2).

In the case of covalent immobilization of protein on the MNP surface using EDC as a coupling agent, there is a risk that a significant excess of this reagent will lead to intramolecular coupling of free functional groups of the protein and, as a result, to a change of its spatial configuration and a decrease of its fluorescent properties. Therefore, we also studied the effect of EDC on the fluorescent properties of TagGFP2. When adding 0.3 mL ($5 \cdot 10^{-5}$ mol L⁻¹) of EDC to 3 mL of an aqueous solution of protein ($6.8 \cdot 10^{-7}$ mol L⁻¹), the opalescence of the sample rapidly increased during the first 15 min and afterwards increased gradually, which is confirmed by an increased background

Scheme 1



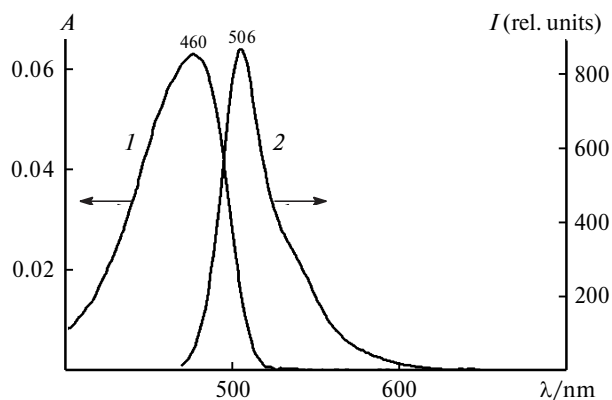


Fig. 1. Absorption (1) and emission spectra (2) of protein TagGFP2.

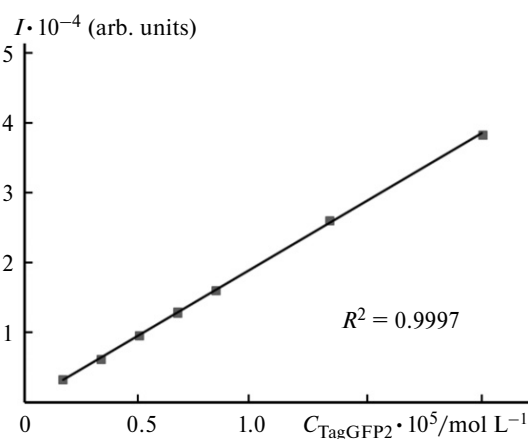


Fig. 2. Calibration curve of the dependence of the area under the luminescence curve in the region of 450–600 nm on protein TagGFP2 concentration.

line in the absorption spectra (Fig. 3, *a*). On the second day, the background line decreased due to precipitation. The precipitation has no effect on the fluorescent properties of the protein solution, therefore, fluorescence spectroscopy is still preferable. In addition, the possibility of varying the voltage at the spectrofluorimeter photomultiplier makes it possible to work at both low (10^{-7} – 10^{-6} mol L $^{-1}$) and higher protein concentrations (up to 10^{-5} mol L $^{-1}$). It was shown that the presence of EDC in the solution leads to a noticeable quenching of TagGFP2 fluorescence, which can be described by a logarithmic dependence (Fig. 3, *b*). This is caused by a change in the protein structure resulting from intra- and, possibly, intermolecular couplings. It is likely that these processes result in the formation of microparticles and their sedimentation. Therefore, in the case of covalent immobilization of TagGFP2 on MNPs **1** and MNPs **2**, we used equimolar amounts of EDC calculated based on the quantity of functional groups on the MNP surface.

The immobilization of TagGFP2 on MNPs **1** was carried out according to Scheme 1.

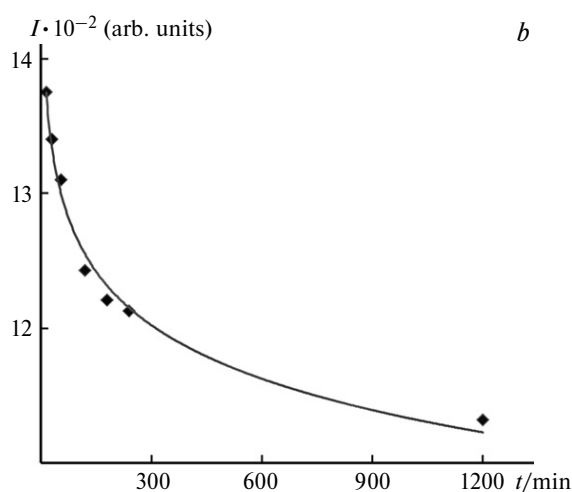
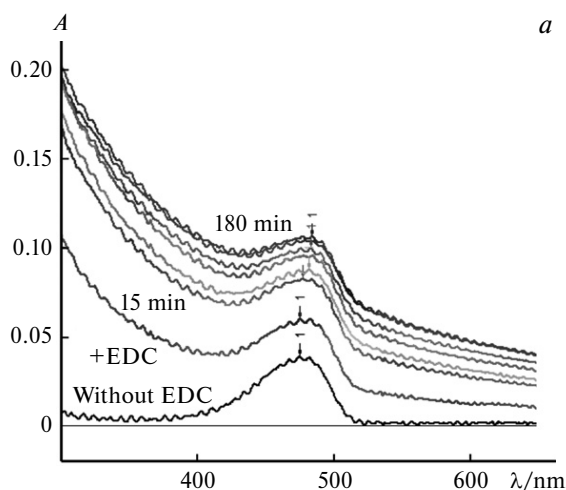


Fig. 3. The change in the absorption spectra (*a*) and the decrease over time in the luminescence intensity of protein TagGFP2 (*b*) after the addition of EDC.

For this purpose, an equimolar amount of EDC was added to a colloidal solution of MNPs **1** in PBS or water (products **3** and **4**, respectively, were obtained during the process), then the mixture was allowed to stand at room temperature for 1 h, followed by the addition of an aliquot of TagGFP2 solution with a molar ratio of carboxy groups on MNPs **1** to the protein 25 : 1 and 75 : 1. In addition, the possibility of non-covalent immobilization of TagGFP2 on MNPs was investigated by carrying out a similar reaction, but in the absence of carbodiimide (product **5**).

The reaction progress was monitored using UV spectroscopy and fluorimetry. The UV and luminescence spectra were recorded when TagGFP2 was just added, and after 0.5, 1, 4, and 20 h. It was shown that UV and luminescence spectra of the sample do not change over time (the maximum difference in the intensity in the spectra was up to 4%). At the same time, the difference in fluorescence intensity in parallel measurements did not exceed 4.5%. This may indicate that the use of carbodiimide does not

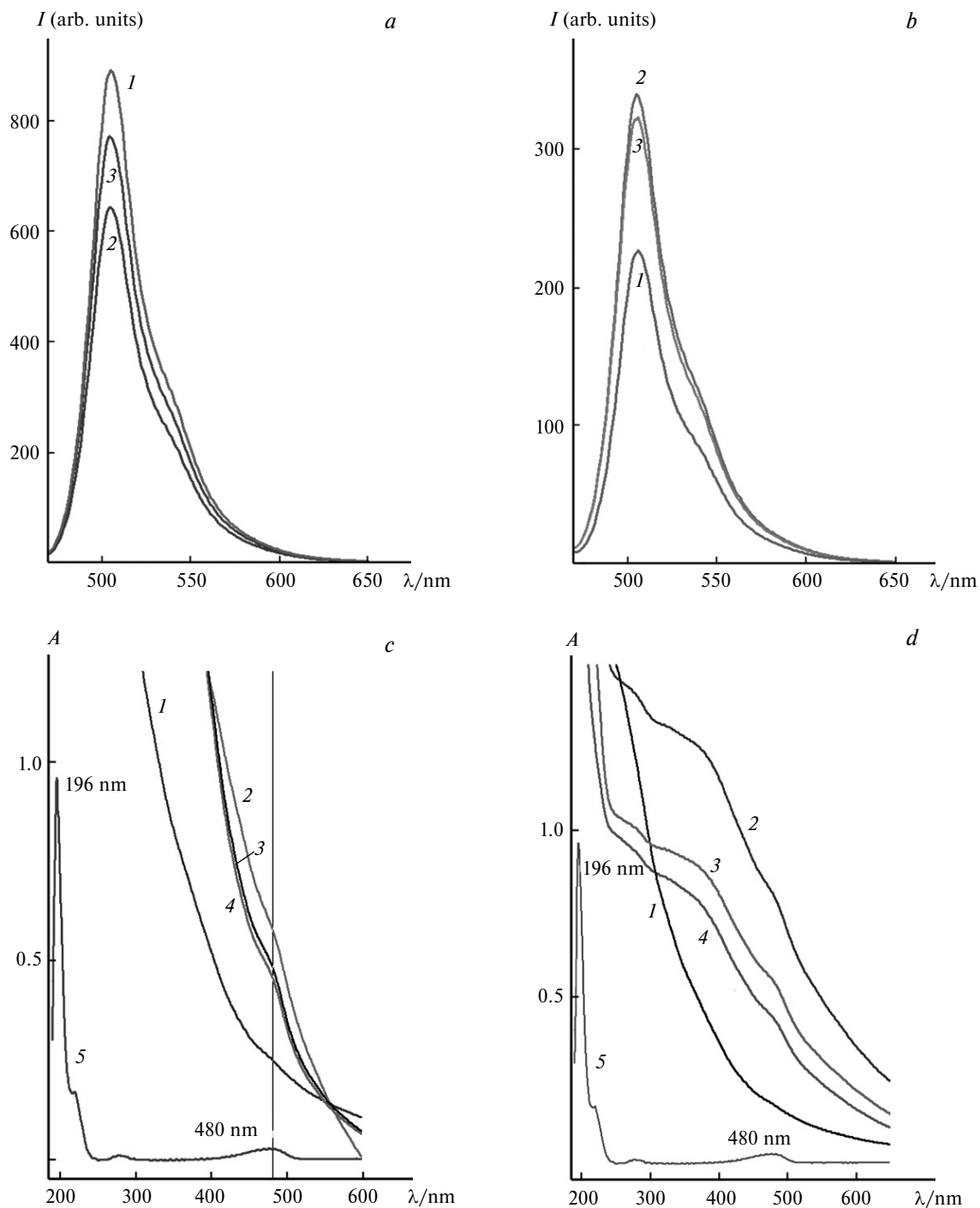


Fig. 4. Luminescence spectra of the reaction mixtures after the completion of the reaction and the removal of nanoparticles for MNPs containing carboxy groups (1–3, MNPs 3–5, respectively) (a), and for MNPs containing amino groups (1–3, MNPs 6–8, respectively) (b), as well as optical absorption spectra of synthesized MNPs for conjugates based on MNPs containing carboxy group (1, MNPs 1, 2–4, MNPs 3–5, respectively, 5, TagGFP2) (c), and for conjugates based on MNPs containing amino groups (1, MNPs 2, 2–4, MNPs 6–8, respectively, 5, TagGFP2) (d).

lead to the loss of fluorescent properties by the protein under the reaction conditions. Figure 4 shows the absorption and fluorescence spectra of the reaction mixtures of MNPs and TagGFP2 for various conjugation conditions (Table 1).

The amount of immobilized TagGFP2 on MNPs was determined by the difference in the amounts of protein loaded to the reaction and protein remaining in the filtrate after the removal of MNPs. The amount of unreacted

Table 1. The amount of TagGFP2 immobilized on MNPs depending on the reaction conditions

MNPs	Medium	EDC/equiv.	Amount of TagGFP2	
			$\mu\text{g mg}^{-1}$ of MNPs	$\mu\text{mol g}^{-1}$ of MNPs
3	PBS	1	40	1.6
4	H ₂ O	1	150	5.5
5	H ₂ O	0	100	3.6
6	PBS	1	40	1.6
7	H ₂ O	1	25	0.9
8	H ₂ O	0	25	0.9

protein was calculated by means of the calibration curve (see Fig. 2), using the data on signal intensity in the sample fluorescence spectra (see Fig. 4, *a*). It was shown that TagGFP2 immobilization efficiency was practically independent of the molar ratio of the amount of carboxy groups on MNPs **1** to the amount of protein added to the reaction (25 : 1 and 75 : 1) and was equal to 1.6 and 1.5 $\mu\text{g mg}^{-1}$ of MNPs, respectively.

Table 1 gives the data on the degree of TagGFP2 immobilization depending on the reaction conditions for MNPs **3–8** obtained in accordance with Scheme 1.

The optical absorption spectra pattern of the synthesized MNPs **3–5** (see Fig. 4, *c*) correspond to the that of the starting MNPs **1** and additionally contains a small maximum in the region of 460–480 nm characteristic of TagGFP2. The immobilization of TagGFP2 on MNPs was also qualitatively confirmed by IR spectroscopy (Fig. 5). Absorption bands corresponding to the starting

components of the reaction, which underwent certain shifts, were observed in the attenuated reflectance spectra (ATR). Specifically, the TagGFP2 is characterized by the bands in the region of 1636–1646 cm^{-1} (amide I) and 1538–1542 cm^{-1} (amide II), which are present in the spectra of all the studied products.²¹ The bands at 1070 and 977 cm^{-1} , corresponding to vibrations of free OH groups, disappear in MNPs **3–5**, probably due to coordination of protein molecules with surface groups of MNPs. Weak bands at 2860, 2926, and 2960 cm^{-1} corresponding to vibrations of C–H bonds become more pronounced in the protein-modified MNPs. The band at 3430 cm^{-1} , related to the stretching vibrations of H₂O molecules present on the surface of the particles, is broader in the spectra of TagGFP2-modified MNPs compared to that of the starting MNPs **1**. This is due to the additional contribution from the stretching vibrations of protein NH₂ groups. The characteristic band of the starting MNPs **1** is the band at 532 cm^{-1} , which corresponds to vibrations of the Fe–O bond. In modified MNPs, it shifts to 547–551 cm^{-1} , which indicates significant surface changes in the MNPs. The broad bands at 1044–1048 cm^{-1} related to vibrations of the P–O bonds,^{17,18} as well as the band corresponding to vibrations of the C=O bond, which undergoes a noticeable shift and superimposes onto the amide I band, remain in the spectra of modified MNPs.

The intensity of almost all the bands for samples **3–5** obtained under different conditions is similar, therefore, it is difficult to evaluate the amount of immobilized protein from ATR spectra. However, one can use a band in the region of 1538–1542 cm^{-1} (amide II) (Fig. 5, *b*), which has a noticeably lower intensity in sample **3** obtained in

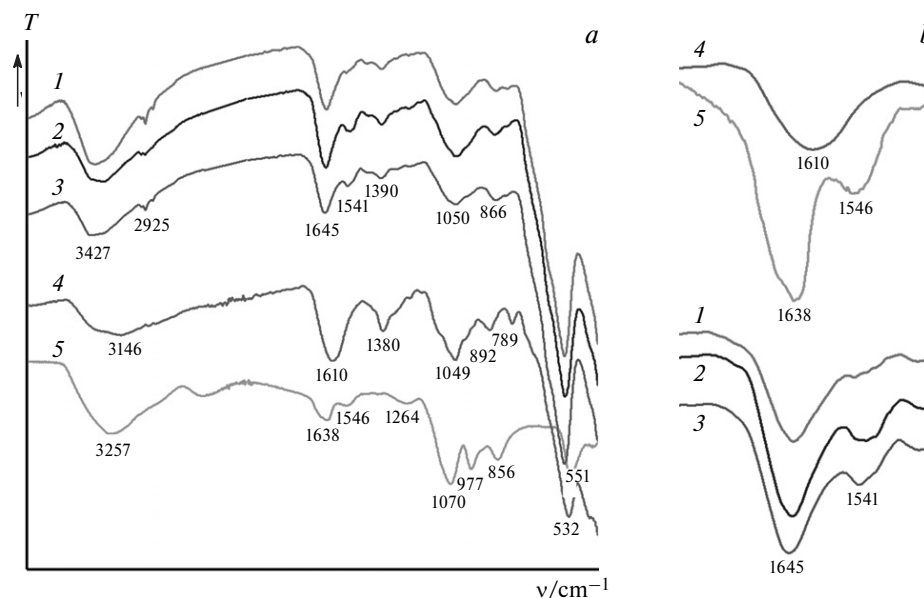


Fig. 5. (*a*) ATR IR spectra of MNPs **1** modified with TagGFP2 in PBS (**1**), in water with the addition of EDC (**2**), in water without EDC (**3**), as well as the starting MNPs **1** (**4**) and TagGFP2 (**5**). (*b*) A zoomed-in section of the spectrum in the region of 1450–1750 cm^{-1} .

PBS. The smallest amount of immobilized protein in sample **3** was confirmed by fluorimetry (see Table 1).

The immobilization of TagGFP2 on MNPs **2** was carried out in accordance with Scheme 1, by analogy with the modification of MNPs **1**. To accomplish this, an equimolar amount of EDC and then TagGFP2 was added to a solution of MNPs **2** in PBS or water (obtaining products **6** and **7**, respectively). In the study of non-covalent sorption, immobilization was carried out without the addition of carbodiimide (obtaining product **8**). Fluorescence spectroscopy was used to measure the amount of TagGFP2 in filtrates after the removal of MNPs from the reaction mixtures. The experimental results are given in Table 1.

The pattern of the optical absorption spectra of the synthesized MNPs **6–8** (see Fig. 4, *d*) corresponded to that of the starting MNPs **2** spectra and additionally contained a small maximum in the region of 460–480 nm characteristic of TagGFP2. The ATR spectra of MNPs **6–8** (Fig. 6) and **3–5** (see Fig. 5) generally are similar. The FTIR spectra of MNPs **6–8** contain absorption bands corresponding to the starting components of the reaction and having undergone shifts: the bands characteristic of TagGFP2 in the region of 1639–1643 cm⁻¹ (amide I), 1530–1539 cm⁻¹ (amide II), and 1383–1394 cm⁻¹ (amide III), and the bands at 2852, 2919, and 2954 cm⁻¹ (C–H stretching vibrations) become more pronounced and better resolved. New (weak, but resolved) bands appear, for example, at 1731–1736 cm⁻¹ (which can correspond to vibrations of free COOH groups in the protein molecule) (see Fig. 6, *b*) and at 1453–1457 cm⁻¹ (amide III). In the spectra of MNPs **6–8**, the band at 545 cm⁻¹ characteristic of the starting MNPs **2** (Fe–O stretching vibra-

tions) shifts toward the region of 543–553 cm⁻¹. There are also broad bands at 1026–1033 cm⁻¹ related to vibrations of Si–O bonds remaining in the spectra of MNPs **6–8**.

Comparing the results on the amount of immobilized protein on MNPs **1** and on MNPs **2**, we can conclude that in H₂O the interaction of TagGFP2 with the surface of negatively charged MNPs **1** occurred six times more efficiently compared to positively charged MNPs **2** (when considering MNPs **4** and **7** obtained under similar conditions).

In both cases, the TagGFP2 molecules are immobilized on MNPs largely non-covalently, by coordinating with surface groups. This is shown in experiments on the immobilization of protein without the addition of a coupling agent to the reaction medium, which could lead to the formation of covalent bonds. In these experiments, the better sorption in H₂O was also observed for a negatively charged surface of MNPs (four times higher for MNPs **5** compared to MNPs **8**).

In the case of MNPs **1**, the addition of carbodiimide leads to an increase in the degree of protein immobilization by 50%, probably, due to covalent binding (see Table 1, MNPs **4** compared to MNPs **5**); in the case of MNPs **2**, the presence of EDC does not affect immobilization (MNPs **7** compared to MNPs **8**).

The buffer PBS (pH 7.4) adversely affects the process of protein immobilization (pI 5.73) on MNPs **1**, apparently, due to a change in the surface charge of the nanoparticles. As a result, the amount of sorbed protein decreases by 73% (compared to MNPs **3** and **4** obtained in PBS and water, respectively). In the case of MNPs **2**, the amount

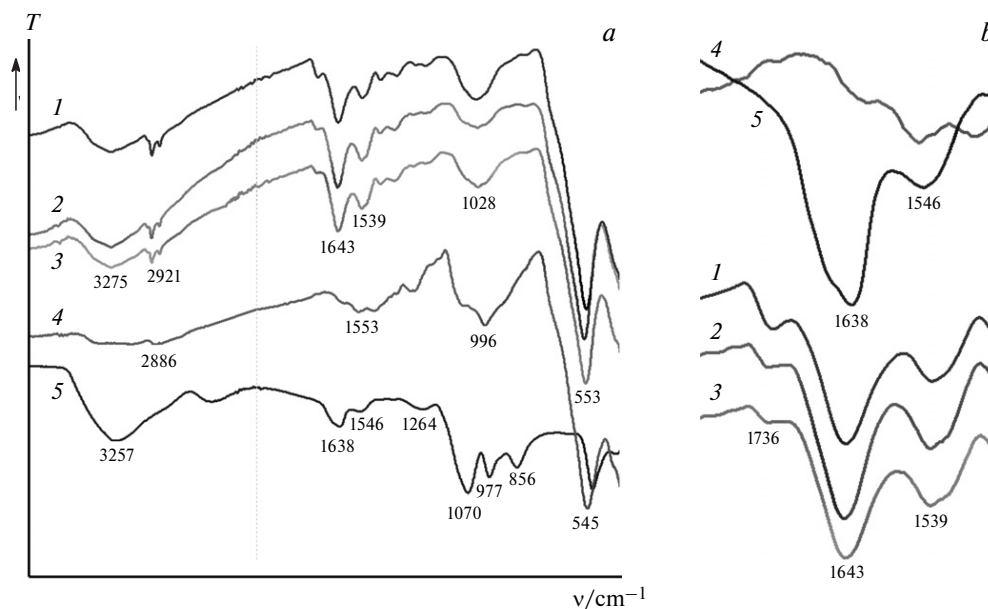


Fig. 6. (a) ATR IR spectra of MNPs **2** modified with TagGFP2 in PBS (**1**), in water with the addition of EDC (**2**), in water without EDC (**3**), as well as the starting MNPs **2** (**4**) and TagGFP2 (**5**). (b) A zoomed-in section of the spectrum in the region of 1450–1750 cm⁻¹.

of TagGFP2, conversely, increases by 60% (compared to MNC 6 and 7).

In conclusion, we studied the immobilization of fluorescent protein TagGFP2 on Fe₃O₄-based MNPs, preliminarily functionalized with PMIDA and APS. It was shown that protein immobilization can occur by both non-covalent and covalent binding mechanisms (when using EDC). The best results were obtained for PMIDA-functionalized MNPs. The use of carbodiimide in this case allows to increase the efficiency of binding TagGFP2 to the surface by up to 50% (when carrying out the reaction in water). This effect was not observed for MNPs 2. Therefore, it can be assumed that the addition of a coupling agent leads to the activation of carboxy groups on the MNP surface, which react with amino groups of the protein, thereby increasing degree of its immobilization. In the case of MNPs 2, on the other hand, it was assumed that the addition of a coupling agent could lead to the activation of free carboxy groups of TagGFP2, which would interact with amino groups on the surface of MNPs. However, since we did not observe an increase in the degree of protein loading, it can be concluded that free amino groups of the protein play a more important role under these conditions of TagGFP2 immobilization.

We believe that the results of this study can contribute to the development of nanomaterials with magnetic and optical properties which can be used as imaging agents for biomedical purposes.

Experimental

Iron(III) chloride hexahydrate (FeCl₃ · 6H₂O, 97%) (Reakhim, Russia) and iron(II) sulfate heptahydrate (FeSO₄ · 7H₂O, 99%) (Vekton, Russia) were used for the synthesis of Fe₃O₄-based MNPs. APTMS (97%) (Alfa Aesar, United Kingdom) and PMIDA (97%) (Sigma-Aldrich, USA) were used for surface modification. 1-(3-Dimethylaminopropyl)-3-ethylcarbodiimide hydrochloride (EDC · HCl, 98%) (Alfa Aesar, United Kingdom) was used as a coupling agent. Dialyzed water (18.2 MΩ cm), phosphate-buffered saline (PBS; 137 mmol L⁻¹ of NaCl, 2.7 mmol L⁻¹ of KCl, 10 mmol L⁻¹ of Na₂HPO₄, 1.8 mmol L⁻¹ of KH₂PO₄, pH 7.4), 95% ethanol were used in the work.

Immobilization of APS and PMIDA, as well as TagGFP2 on MNPs, was confirmed by IR spectroscopy. The IR spectra were recorded on a Nicolet-6700 infrared Fourier-transform spectrometer (Thermo Electron Corporation) equipped with a Smart Orbit diamond ATR accessory. The scanning region of ATR spectra was 400–4000 cm⁻¹, the number of scans was 64. The mass fraction of carbon was determined using an automatic PE-2400 CHN analyzer, series II (Perkin Elmer). Fluorimetry (Cary Eclipse spectrofluorometer, Varian) and UV spectroscopy (UV 2401 PC spectrophotometer, Shimadzu) were used to determine the amount of immobilized protein, the region of registration was 190–1100 nm).

To plot the calibration curve, distilled water (3 mL) was added to a quartz cell using a dispenser. Then, protein solution in PBS (from 1 to 50 μL) at a concentration of 2 mg mL⁻¹ was

added with a dispenser. The absorption and luminescence spectra were recorded at an excitation wavelength of 460 nm for each sample. Using the collected data, a graph of the area under the luminescence curve in the region of 450–600 nm *versus* concentration was plotted. The concentration *C* (mol L⁻¹) was calculated using the formula

$$C(\text{mol L}^{-1}) = C(\text{mg mL}^{-1}) \cdot A / (27000 \cdot 3),$$

where *A* is the aliquot in mL, 27000 is the molecular mass of the protein, 3 is the volume of distilled water in the cell (mL).

In further experiments, the data on the luminescence of the samples under study were used to determine the protein concentration (mol L⁻¹) based on the calibration curve (see Fig. 2).

Synthesis procedure of Fe₃O₄ MNPs. Synthesis of MNPs was carried out according to a previously published procedure.^{15,16} Saturated ammonia solution (3 mL) was added to a solution of FeSO₄ · 7H₂O (0.278 g, 1.0 mmol) and FeCl₃ · 6H₂O (0.541 g, 2.0 mmol) in water (10 mL) with stirring by a mechanical stirrer and treatment with ultrasound until pH 11 was reached. After 30 min, the MNPs were precipitated using an external magnet and washed with deionized water to pH 7. The obtained MNPs were stored as an aqueous colloidal solution. According to transmission electron microscopy (TEM) results (Philips CM30, FEL, Netherlands), the phase composition of the obtained nanoparticles corresponded to magnetite, the average particle diameter was 11 nm. The specific magnetization of saturation was 80 Gs cm³ g⁻¹ (vibration magnetometer with a magnetic field up to 2.2 mA m⁻¹, IMP UrB, Russia).

Synthesis procedure of MNPs 1. Synthesis of MNPs 1 was carried out according to a previously published procedure.^{17,18} A solution of PMIDA (0.286 g) in water (100 mL) was added to a suspension of MNPs in water (135 mL, a concentration of 2 mg mL⁻¹) (4.3 mmol of PMIDA per 1 g of MNPs) with stirring. After 1 day, the resulting suspension was centrifuged for 10 min at 5000 rpm (to remove large particles), then 10 min at 17000 rpm (to remove excess PMIDA). The precipitate was re-suspended in water to obtain a suspension of MNPs 1 with a concentration of 1.2 mg mL⁻¹. The amount of carboxy groups on the surface of MNPs was 0.57 mmol per 1 g of MNPs.

Synthesis procedure of MNPs 2. Synthesis of MNPs 2 was carried out according to a previously published procedure.^{15,16} A solution of APTMS (142 μL) in EtOH (15 mL) was added to a suspension of MNPs in EtOH (135 mL, a concentration of 2 mg mL⁻¹) (3 mmol of APTMS per 1 g of MNPs) with stirring. After 1 day, MNPs 2 were precipitated in a magnetic field, washed with EtOH and water, re-suspended in water using ultrasound to obtain a colloidal solution of MNPs 2 with a concentration of 4.0 mg mL⁻¹. The amount of amino groups on the surface of MNPs was 0.60 mmol per 1 g of MNPs.

Immobilization of TagGFP2 on MNPs 1 (3–5) (general procedure). To obtain MNPs with TagGFP2 protein immobilized on their surface, water (or PBS) (4.0 mL) was added to a suspension of MNPs 1 (0.14 mL, 0.17 mg, 1.9 · 10⁻⁷ mol of COOH groups) and the mixture was treated with ultrasound for 3 min. Then, a freshly prepared aqueous solution of EDC · HCl (0.20 mL, 7.4 · 10⁻⁹ mol) was added and the mixture was allowed to stand for 1 h. A solution of TagGFP2 (0.10 mL, 0.20 mg, 7.4 · 10⁻⁹ mol) was added to the suspension with activated MNPs; the reaction mixture was kept for 4 h at room temperature (~25 °C) and then for 12 h at 4 °C. Afterwards, MNPs were precipitated by an external magnetic field, washed with water, precipitated,

and redispersed in water (1.5 mL). The absorption and luminescence spectra of the filtrates were recorded.

Immobilization of TagGFP2 on MNPs 2 (6–8) (general procedure). To immobilize TagGFP2 on MNPs, water (or PBS) (4.0 mL) was added to a suspension of MNPs 2 (0.06 mL, 0.24 mg, $1.7 \cdot 10^{-7}$ mol of NH₂ groups) and the mixture was treated with ultrasound for 3 min. Afterwards, a freshly prepared aqueous solution of EDC (0.05 mL, $1.7 \cdot 10^{-7}$ mol) was added. A solution of TagGFP2 (0.10 mL, 0.20 mg, $7.4 \cdot 10^{-9}$ mol) was added to the obtained suspension of MNPs; the reaction mixture was allowed to stand for 4 h at 25 °C and then for 12 h at 4 °C. The nanoparticles were precipitated by an external magnetic field, washed with water, precipitated, and redispersed in water (1.5 mL). The absorption and luminescence spectra of the filtrates were recorded.

TagGFP2 production. The recombinant protein TagGFP2 containing six histidine residues (His6-tag) at the N-terminus was expressed in *E. coli* cells (Rosetta DE3) transformed by a plasmid vector pQe-30-TagGFP2 (Evrogen, Russia) according to the standard protocol.²² The protein was purified by metal chelate chromatography, using Ni-NTA-agarose (Qiagen, Germany). The purity (<95%) and correspondence of the molecular weight of the isolated protein (28 kDa) were determined by denaturing gel electrophoresis in polyacrylamide gel with an addition of sodium dodecylsulfate (SDS-PAGE).²³ The concentration of protein TagGFP2 was determined using the Bradford method,²⁴ bovine serum albumin (Sigma) was used as the standard.

The study was conducted using the equipment of the Center for Joint Use "Spectroscopy and Analysis of Organic Compounds".

This work was financially supported by the Russian Science Foundation (Project No. 14-15-00247). Fluorimetry studies were performed within the framework of the State assignment theme (AAAA-A19-119011790130-3).

References

1. O. Veisoh, J. Gunn, M. Zhang, *Adv. Drug Deliv. Rev.*, 2010, **62**, 284.
2. C. Xu, S. Sun, *Adv. Drug Deliv. Rev.*, 2013, **65**, 732.
3. S. Laurent, D. Forge, M. Port, A. Roch, C. Robic, L. Vander Elst, R. N. Muller, *Chem. Rev.*, 2008, **108**, 2064.
4. Y.-X. J. Wang, *Quant. Imaging Med. Surg.*, 2011, **1**, 35.
5. J. Gao, H. Gu, B. Xu, *Acc. Chem. Res.*, 2009, **42**, 1097.
6. A. M. Demin, Yu. V. Kuznetsova, V. P. Krasnov, A. A. Rempel, *Dokl. Chem.*, 2016, **467**, 113.
7. A. M. Demin, M. V. Ulitko, A. S. Minin, Yu. V. Kuznetsova, S. V. Rempel, V. P. Krasnov, A. A. Rempel, *Dokl. Chem.*, 2016, **467**, 118.
8. C.-W. Hung, T. Holomana, P. Kofinas, W. E. Bentley, *Biochem. Eng. J.*, 2008, **38**, 164.
9. I. F. Nata, N. S. El-Safory, C. K. Lee, *ACS Appl. Mater. Interfaces*, 2011, **3**, 3342.
10. I. S. Lee, N. Lee, J. Park, B. H. Kim, Y.-W. Yi, T. Kim, T. K. Kim, I. H. Lee, S. R. Paik, T. Hyeon, *J. Am. Chem. Soc.*, 2006, **128**, 10658.
11. B. J. Kim, Y. Piao, N. Lee, Y. Park, I.-H. Lee, J.-H. Lee, S. R. Paik, T. Hyeon, *Adv. Mater.*, 2010, **22**, 57.
12. S. Engin, V. Trouillet, C. M. Franz, A. Welle, M. Bruns, D. Wedlich, *Langmuir*, 2010, **26**, 6097.
13. Z.-F. Gan, J.-S. Jiang, Y. Yang, B. Du, M. Qian, P. Zhang, *J. Biomed. Mater. Res. A.*, 2008, **84A**, 10.
14. O. M. Subach, I. S. Gundorov, M. Yoshimura, F. V. Subach, J. Zhang, D. Grünwald, E. A. Souslova, D. M. Chudakov, V. V. Verkhusha, *Chem. Biol.*, 2008, **15**, 1116.
15. A. M. Demin, A. G. Pershina, K. V. Nevskaya, L. V. Efimova, N. N. Shchegoleva, M. A. Uimin, D. K. Kuznetsov, V. Ya. Shur, V. P. Krasnov, L. M. Ogorodova, *RSC Adv.*, 2016, **6**, 60196.
16. A. M. Demin, A. G. Pershina, V. V. Ivanov, K. V. Nevskaya, O. B. Shevelev, A. S. Minin, I. V. Byzov, A. E. Sazonov, V. P. Krasnov, L. M. Ogorodov, *Inter. J. Nanomed.*, 2016, **11**, 4451.
17. A. M. Demin, A. V. Mekhaev, A. A. Esin, D. K. Kuznetsov, P. S. Zelenovskiy, V. Y. Shur, V. P. Krasnov, *Appl. Surf. Sci.*, 2018, **440**, 1196.
18. A. M. Demin, A. G. Pershina, A. S. Minin, A. V. Mekhaev, V. V. Ivanov, S. P. Lezhava, A. A. Zakharova, I. V. Byzov, M. A. Uimin, V. P. Krasnov, L. M. Ogorodova, *Langmuir*, 2018, **34**, 3449.
19. A. M. Demin, A. G. Pershina, V. V. Ivanov, O. B. Shevelev, M. A. Uimin, K. V. Nevskaya, N. N. Shchegoleva, A. S. Minin, A. E. Sazonov, V. P. Krasnov, L. M. Ogorodova, *Izv. Vuzov. Fiz. [Bull. of Higher Inst. Phys.]*, 2015, **58**, No. 12/2, 68 (in Russian).
20. A. M. Demin, O. V. Koryakova, V. P. Krasnov, *J. Appl. Spectr.*, 2014, **81**, 565.
21. H. Fukuda, M. Arai, K. Kuwajima, *Biochemistry*, 2000, **39**, 12025.
22. T. Maniatis, E. F. Fritsch, J. Sambrook, *Molecular Cloning: A Laboratory Manual*, Cold Spring Harbor Laboratory Press, New York, 1982, 2230 pp.
23. U. K. Laemmli, *Nature*, 1970, **227**, 680.
24. M. M. Bradford, *Anal. Biochem.*, 1976, **72**, 248.

Received October 12, 2018;
accepted March 21, 2019